ACS EARTH AND SPACE CHEMISTRY

http://pubs.acs.org/journal/aesccq

Article

Acyclic Terpenes Reduce Secondary Organic Aerosol Formation from Emissions of a Riparian Shrub

Farzaneh Khalaj, Albert Rivas-Ubach, Christopher R. Anderton, Swarup China, Kailen Mooney, and Celia L. Faiola*

Cite This: *ACS Earth Space Chem.* 2021, 5, 1242−1253

Read Online

ACCESS | Metrics & More | Article Recommendations | Supporting Information

ABSTRACT: Terrestrial vegetation is a major global source of atmospheric secondary organic aerosol (SOA) through oxidation of biogenic volatile organic compound (BVOC) emissions. Climate change is altering the composition of BVOC emissions by increasing the prevalence of plant stress conditions, such as frequency and intensity of herbivorous insect outbreaks. The impact this will have on SOA formation is unknown. This laboratory study investigated the influence of aphid herbivory (*Uroleucon macolai*) on SOA formation from emissions of a common riparian shrub in California, *Baccharis salicifolia* (Asteraceae). Aphid herbivory increased the relative contribution of *β*-ocimene and decreased the relative contribution of *β*-guaiene in the BVOC emission profile. These effects on BVOC emissions did not translate to a significant aphid effect on SOA mass yields. However, for both control and aphid experiments, the fraction of total acyclic monoterpenes in the BVOC emission profile was correlated with reduced SOA mass yield. This is the first study to demonstrate a clear reduction in SOA mass yield as the proportion of acyclic terpenes in a complex BVOC mixture increased. These findings highlight the importance of better understanding acyclic terpene chemistry in the atmosphere to improve predictions of SOA in both current and future climates.

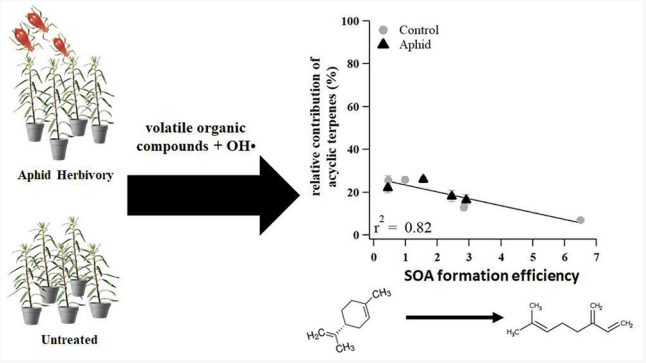

KEYWORDS: *secondary organic aerosol, biogenic volatile organic compounds, plant−atmosphere interactions, atmospheric chemistry, plant stress*

1. INTRODUCTION

Plants produce over one million different chemical metabolites[1] of which at least 1000 are emitted to the atmosphere as biogenic volatile organic compounds (BVOCs).[2,3] These compounds are highly reactive and participate in important atmospheric aerosol processes including particle nucleation[4] and secondary organic aerosol (SOA) formation,[5] whereby they influence aerosol climate effects by altering particle composition,[6−8] hygroscopicity,[9] and optical properties.[10−12] Plant BVOCs, particularly terpenes, are the largest contributor to atmospheric SOA globally.[13,14] The SOA chemistry of a few common terpene compounds (i.e., isoprene, *α*-pinene, *β*-pinene, limonene) has been studied extensively in laboratory chamber experiments,[15−18] and this seminal work has provided the foundation for model predictions of SOA production. However, these laboratory experiments represent a small fraction of all BVOCs, which have a diverse range of molecular structures with atmospheric reactivity varying by orders of magnitude even between different types of terpenes.[19,20] The types of BVOCs emitted by plants (or the BVOC emission profile) varies in different environmental contexts[21] and between different plant species,[22] many of which are undergoing substantial range shifts due to climate change.[23] This presents unique challenges for improving SOA predictions in a rapidly changing world where future spatiotemporal distributions of BVOC profiles could look very different from today. Addressing this challenge necessitates a more complete understanding of the aerosol chemistry associated with these highly complex plant volatile mixtures across a range of environmental conditions.

Each step of the SOA formation process, from BVOC emissions to atmospheric chemistry, is affected by a changing climate, leading to unpredictable BVOC-aerosol-vegetation climate feedbacks. For example, increased temperature and atmospheric carbon dioxide are both predicted to increase BVOC emission rates with subsequent increases in SOA

Special Issue: Chemical Interactions in the Plant-Atmosphere-Soil System

Received: October 29, 2020
Revised: March 10, 2021
Accepted: March 22, 2021
Published: April 8, 2021

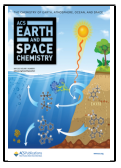

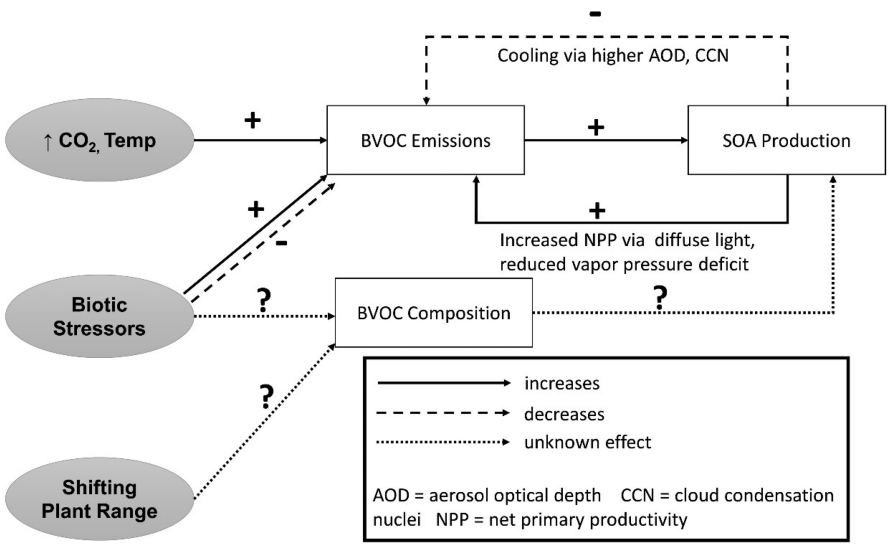

Figure 1. Simplified schematic of the BVOC-aerosol-vegetation feedback associated with changing BVOC emission rates and BVOC composition. We have not included all of the potential sources that could change BVOCs but rather provide a sample to illustrate the process.

production.[24−26] Increased SOA can have two very different effects on plant physiology and BVOC emission rates. The first effect is to reduce BVOC emissions (negative feedback) through aerosol radiative cooling that results from increased aerosol optical depth and increased number of cloud condensation nuclei.[27] This occurs because BVOC emission rates are exponentially related to temperature so any radiative cooling effect will decrease BVOC emission rates.[28] The second effect is to increase BVOC emissions (positive feedback) through increased plant net primary productivity driven by increased diffuse photosynthetic radiation and decreased vapor pressure deficit. The existence of the positive feedback effect has been supported with both modeling[29] and field observations,[30] although there are still questions about the net BVOC-aerosol-vegetation feedback effect due to the inherent complexity of this system.[31] Accounting for both positive and negative feedback effects, the Norwegian Earth System Model estimates a net negative radiative forcing of −0.49 W m^{-2} offsetting 13% of forcing associated with doubling atmospheric CO_2.[32] These results highlight that the BVOC-aerosol-vegetation feedback is worthy of further investigation, including the consideration of important factors other than temperature and CO_2 that could alter BVOC emissions. For example, it could be of equal or greater importance that many abiotic and biotic plant stressors alter both the BVOC emission profile and emission rates,[33−37] and that plant species are currently undergoing drastic range shifts altering the distribution of plant types across Earth's surface.[23] Both of these will change the spatiotemporal distribution of atmospheric BVOC composition. A simplified schematic illustrating this BVOC-aerosol-vegetation feedback is shown in Figure 1. Note that "biotic stressors" can include insect herbivory and pathogens, which could increase BVOC emissions in the short term but could also decrease BVOC emissions in the long term depending on severity and plant mortality. Currently, there are major gaps in our understanding of how BVOC composition could change in the future and how this could influence SOA production.

Changes in BVOC composition from different plant species can alter SOA formation through effects on nucleation rates and condensational growth. Ozonolysis of plant BVOC emission profiles with a higher contribution of sesquiterpenes (e.g., loblolly pine, *Pinus taeda*) generated much higher particle formation rates than plant systems dominated by monoterpene emissions (e.g., holm oak, *Quercus ilex*).[38] Similarly, new particle formation was enhanced via photooxidation of birch (*Betula pendula*) emissions containing high amounts of oxygenated BVOCs (e.g., 3-hexenol, 3-hexenyl acetate, and methyl salicylate) compared to pine (*Pinus sylvestris*) and spruce (*Picea abies*) emissions.[39] All of these examples demonstrate that variations in the complex mixtures of BVOCs from different plants produce variations in aerosol formation but plant BVOC emission profiles of individuals from the same plant species can also change when a plant experiences stress.

Plant stress can increase SOA production, for example, due to insect herbivory or mechanical wounding.[40−42] Part of the increase in SOA production observed in laboratory chamber experiments is simply due to large increases in BVOC emission rates where increased emissions lead to increased BVOC mixing ratios in the laboratory reaction chamber and higher SOA mass. Of equal interest is the effect of plant stress on SOA yield, which is more nuanced and can vary from plant system to plant system depending on how the BVOC composition is affected by the stress. For example, some plant stressors preferentially increase emissions of monoterpenes over sesquiterpenes, effectively reducing the sesquiterpene-to-monoterpene ratio, leading to decreases in SOA mass yield.[40] Other stressors increase emissions of large cyclic sesquiterpenes or large oxygenated compounds like methyl salicylate, which increase SOA mass yields[43] and decrease hygroscopicity of the resulting particles.[9] None of these plant stress effects on SOA formation are accounted for in global climate models, and their importance for the BVOC-aerosol-vegetation feedback have not been investigated. Currently, there are not enough laboratory SOA studies using real plant emissions to identify the key chemical features in these changing BVOC mixtures that drive SOA formation and climate-relevant properties.

In this study, we investigated the effects of insect herbivory on SOA formation from a common riparian shrub in California, *Baccharis salicifolia*. Plants were exposed to a

https://doi.org/10.1021/acsearthspacechem.0c00300
ACS Earth Space Chem. 2021, 5, 1242−1253

specialist sap-feeding aphid herbivore that only feeds on this genus of plant, and emissions from control and aphid-treated plants were used to generate SOA in the laboratory with an oxidation flow reactor. BVOCs were sampled during each SOA experiment to allow us to identify the specific chemical features in the complex mixture that were driving SOA production in the flow reactor. Leaf samples were collected at the completion of the experiment for foliar metabolome analysis to evaluate the effect of aphid herbivory on plant health. To our knowledge, this is the first laboratory study investigating effects of insect herbivory on SOA formation from shrubs, which dominate the vegetation landscape in many regions including the coastal sage scrub and chapparal in California.

2. EXPERIMENTAL METHODS

2.1. Experiment Overview. SOA was generated in the laboratory by oxidizing the emissions of 4−11 plants located inside a Teflon plant enclosure. Multiple plants were required to generate a measurable amount of SOA mass (e.g., condensed phase organic aerosol mass). Each set of plants was used to conduct an SOA "trial", which refers to the generation of an SOA mass yield curve with at least 3−4 SOA yield data points for each curve. The SOA mass yield curves were used to compare SOA formation efficiency between the trials. Experimental replicates were defined as the SOA trial, meaning each SOA mass yield curve constructed from multiple SOA mass loadings is a single replicate (Table 1). Each trial was both time and labor intensive, so replicates were thus restricted to four control trials and four aphid treatment trials. Each aphid trial used 4−5 plants, and each control trial used 8−11 plants. More control plants had to be used to obtain the same SOA mass range because emission rates were likely lower than aphid-exposed plants (as expected). A more detailed description of the methods used for SOA generation is provided in Section 2.3. BVOCs were collected for each condensed mass loading in the SOA trial, but the average BVOC emission profile was used for subsequent volatile analysis and statistics. Leaves were harvested from each plant after the SOA trial was completed to evaluate the effect of the aphid treatment on plant health via its effects on the foliar metabolome. The timing of the treatment and control SOA trials was dependent on plant availability. We note that we were unable to use a randomized block design due to this and consequently all herbivore-treatment SOA trials were performed first followed by all control trials (see dates in Table 1). We acknowledge that there was a time variable separating aphid trials from control trials that we could not necessarily pull out due to the timing of plant availability where all aphid trials were conducted first followed by all control trials. To assess whether the temporal clustering of the trials from the two treatments may have affected our results, we inspected whether variation in the timing of trials within a treatment group differed. This was not the case (see Section 3.1), leading us to conclude that little, if any, of the treatment effects observed were attributable to the sequencing of the trials.

2.2. Plants and Aphid Herbivore Treatment. *Baccharis salicifolia* (Asteraceae) is a woody dioecious shrub native to the southwestern United States and Northern Mexico. Plant cuttings were collected at a field site in the University of California Natural Reserve System San Joaquin Marsh Reserve (33.65°N, 117.85°E; Orange County, CA, U.S.A.). BVOC emission profiles in *Baccharis salicifolia* are independent of plant sex, so cuttings were collected from both plant sexes and

Table 1. Summary of Information for Each SOA Mass Yield Curve Data Point from Each SOA Trial[a]

trial ID	date	point[b]	RH (%)	$BVOC_i$[c]	C_{OA}[c]	OH_{exp}[d]
aphid 1	03/28/2018	1	58	35	1.4	8.1×10^{11}
		2	55	34	0.8	$7{,}8 \times 10^{11}$
		3	50	33	0.4	7.4×10^{11}
aphid 2	04/04/2018	1	70	112	2.5	8.5×10^{11}
		2	68	123	2.7	8.0×10^{11}
		3	60	92	1.8	7.8×10^{11}
		4	55	70	1.1	7.7×10^{11}
aphid 3	05/02/2018	1	80	53	2.1	9.7×10^{11}
		2	80	47	1.4	9.7×10^{11}
		3	75	44	0.9	9.4×10^{11}
		4	70	33	0.5	9.1×10^{11}
aphid 4	05/08/2018	1	75	36	2.7	9.4×10^{11}
		2	80	37	1.9	9.7×10^{11}
		3	85	32	0.9	9.8×10^{11}
control 1	05/16/2018	1	75	15	0.8	9.6×10^{11}
		2	73	16	0.6	9.5×10^{11}
		3	65	14	0.5	8.8×10^{11}
		4	60	15	0.3	8.4×10^{11}
control 2	05/18/2018	1	80	37	2.7	9.8×10^{11}
		2	75	46	1.6	9.3×10^{11}
		3	75	44	1.4	9.4×10^{11}
		4	70	43	0.6	9.0×10^{11}
control 3	05/22/2018	1	60	150	2.7	7.5×10^{11}
		2	55	160	2.6	7.0×10^{11}
		3	50	110	0.9	6.8×10^{11}
		4	45	67	0.5	6.8×10^{11}
control 4	05/24/2018	1	55	190	2.4	6.8×10^{11}
		2	45	147	1.7	6.8×10^{11}
		3	40	66	0.9	6.8×10^{11}
		4	39	76	0.4	6.8×10^{11}

[a]Including date of experiment, relative humidity (RH) in OFR, mass concentration of BVOCs introduced to the OFR ($BVOC_i$), mass concentration of condensed organic aerosol formed in the OFR (C_{OA}), and OH exposure (OH_{exp}). [b]Points, refers to the point number for the SOA mass yield curve in that SOA trial. [c]Units are $\mu g\ m^{-3}$. [d]Units are molecules $cm^3\ s^{-1}$.

used for the experiment.[44] We imposed an herbivore treatment by an aphid species known to induce changes in *Baccharis salicifolia* volatile emissions.[44] The aphid used in this study, *Uroleucon macolai*,[45] is a dietary specialist herbivore feeding only on two *Baccharis* species, including *Baccharis salicifolia*. Like all aphids, this species is sap-feeding, viviparous, parthenogenetic, and thus has a very short generation time (5−10 days).[46] The aphid laboratory colony, collected in the Marsh reserve, was sourced from a single cluster of aphids and was thus likely to all be of a single genotype.

The *Baccharis salicifolia* stems were cut from mature plants in October 2017. Individual plant stems (from the same plant source cut) were grown in 4 in. pots in a 1:1:1:1 mixture of sand, peat moss, redwood compost, and pumice garden soil in the greenhouse at the University of California, Irvine. In April 2017, plants were randomly selected for aphid colonization and populations were allowed to grow to about 50 individual aphids. To prevent aphid movement to control plants, plants from aphid and control groups were kept in separate greenhouse rooms of an identical size and maintained under consistent environmental conditions. The aphids were introduced to the plants about one month before aphid SOA

https://doi.org/10.1021/acsearthspacechem.0c00300
ACS Earth Space Chem. 2021, 5, 1242−1253

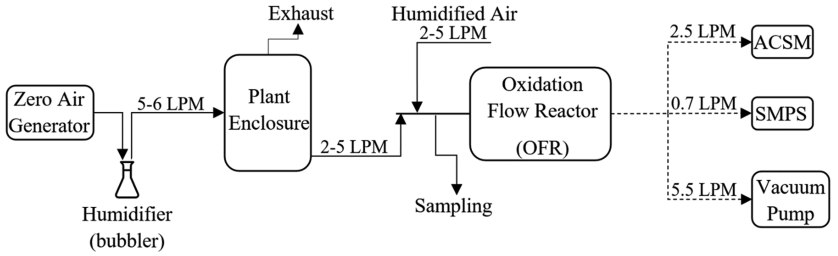

Figure 2. A schematic of the experiment setup. Solid lines refer to PFA tubing and dashed lines refer to copper tubing. LPM refers to liter per min. "Sampling" denotes the location of volatile sampling. ACSM = aerosol chemical speciation monitor and SMPS = scanning mobility particle sizer

experiments were conducted. Before transferring plants to the laboratory to conduct an SOA trial, aphids were removed from plants with a soft brush followed by a gentle water rinse. This was done to eliminate any volatile emissions that might come from the aphids themselves. To account for any effect of the washing treatment, control plants were subjected to the same washing procedure.

2.3. SOA Generation and BVOC Emission Profile Characterization. SOA trials were conducted in a laboratory at University of California, Irvine. Plants were transported from the greenhouse to a custom-built ∼500 L plant enclosure constructed from Teflon sheets and supported by a 1.0 m × 0.7 m × 0.5 m plastic frame. Plants were acclimated to laboratory conditions for a minimum of 24 h to ensure emissions were not elevated due to physical disturbance associated with transportation and the aphid removal processes, which has been shown to be long enough for plant emissions to return to baseline levels.[47] Each trial consisted of generating SOA at a minimum of three different mass loadings to generate an SOA mass yield curve (number of measurement points included in each SOA trial for different replicate sets is shown in Table 1). Aerosol mass loadings <5 $\mu g\ m^{-3}$ were targeted to stay within an atmospherically relevant range in remote areas; the typical range of global ambient biogenic SOA mass loadings vary from 0.1 to 20 $\mu g\ m^{-3}$.[48−50]

SOA was generated via photooxidation of *Baccharis salicifolia* volatile emissions in an oxidation flow reactor (OFR; Aerodyne, Inc.) using the setup shown in Figure 2. Humid clean air was introduced into the plant enclosure continuously with flow rate ranging between 5 to 6 L min^{-1}. Clean air was generated with a zero-air generator (Environics Series 7000) and humidified by passing the air through a bubbler. The plant volatiles were pulled from the plant enclosure headspace into the OFR through 0.25 in PFA tubing at flow rates ranging between 2 to 5 L min^{-1}. This flow rate was controlled by the difference in flow rates between the actively controlled OFR inlet and outlet flows. Humidified air was introduced to the OFR at the inlet and controlled with a mass flow meter between a range of 2.0 to 5.0 L min^{-1}. This range in flows reflect the values required to generate SOA at multiple different mass loadings to generate the SOA mass yield curve. Total flow rate through the OFR was controlled via the outlet flows, which consisted of instrument sampling and an additional vacuum pump flow. Particle size distributions and particle composition were continuously monitored at the outlet with a scanning mobility particle sizer (SMPS; custom-built from TSI, Inc. and Brechtel Inc. components) and time-of-flight aerosol chemical speciation monitor (ToF-ACSM: Aerodyne, Inc.), respectively. The ToF-ACSM sampling line was a 2 m, 3/8″ copper tube that pulled 2.5 L min^{-1} from the same sampling line that served the SMPS. The SMPS pulled 0.7 L min^{-1} with 0.25 in copper tubing. An extra vacuum flow at the outlet was established with a vacuum pump (Thomas, Model 617CA22) and controlled with a needle valve at a flow rate of 5.5 L min^{-1}. Total OFR outlet flow was 8.7 L min^{-1} with a corresponding residence time of 1.49 min. For each SOA mass loading, BVOCs were collected at the OFR inlet on stainless steel adsorbent cartridges containing quartz wool, Tenax TA, and carbograph 5TD (Markes International, Inc.) by pulling 0.42 L min^{-1} through duplicate cartridges in parallel for 4−6 min. Cartridges were capped and stored in a refrigerator until they could be analyzed off-line with a thermo-desorption gas chromatograph mass spectrometer (TD-GC-MS, TD: Markes International Series 2 Unity/Ultra, GC-MS: Agilent GC 7890B with flame ionization detector (FID), equipped with a 30 m, DB-5 column and a Markes, International mass spectrometer BenchTOF-Select type). Details of the GC operation, volatile quantitation and identification are provided in the BVOC emission profile characterization section of Supporting Information (Section 1).

The Aerodyne OFR has been described in detail elsewhere,[51,52] and we include a brief description of the OFR setup we used here. It is a 13 L (45.7 cm length OD × 19.7 cm ID) aluminum cylinder equipped with two low-pressure mercury 185 and 254 nm lamps (BHK, Inc., model no. 82-904-03) to produce OH radicals through the photolysis of H_2O, O_2, and O_3. In our experiment, the OFR was operated using both 185 and 254 nm lamps (referred to as OFR185 mode) in which OH radicals were produced inside the OFR via reaction of oxygen ($O(^1D)$) radicals with water vapor. The ozone (O_3) was generated within the reactor via UV photolysis of oxygen (O_2) with 185 nm lamps. Then oxygen ($O(^1D)$) radicals were produced by UV photolysis of O_3 with the 254 nm lamps inside the reactor. The OH radicals readily react with BVOCs to generate SOA. Before each SOA trial, the OFR was cleaned by flushing overnight with zero air with OFR lights on, and the SMPS and ToF-ACSM were used to verify the reactor was clean before introducing volatiles to the reactor. The ToF-ACSM operating principles, calibration procedures, and analysis protocols are described in detail elsewhere.[53]

A summary of all SOA trials, including treatment group, date conducted, and other relevant details is given in Table 1. For each SOA trial mass yield point, the OFR relative humidity (RH) and plant volatile concentration at the inlet of the OFR were recorded (Table 1). Each SOA trial used volatiles from the same set of plants in the enclosure and was completed in a single day with each SOA mass loading requiring ∼60−90 min to stabilize the system, collect the volatile cartridge samples, and provide a minimum of 10 min averaging interval from the SMPS and ToF-ACSM before and after cartridge sampling. SOA yield was measured at multiple mass loadings to generate

https://doi.org/10.1021/acsearthspacechem.0c00300
ACS Earth Space Chem. 2021, 5, 1242−1253

an SOA mass yield curve. An SOA mass yield curve is a plot of aerosol mass yield versus total condensed organic mass and is a common approach to characterize the SOA formation efficiency of a volatile/oxidant system.[54−59] The SOA mass yield is calculated as the condensed organic aerosol mass generated (ΔC_{OA}) divided by the mass of gas-phase BVOCs that reacted (ΔBVOC). The BVOC concentration at the OFR inlet ranged between 14 to 190 $\mu g\ m^{-3}$. The conditions in the OFR were targeted to be as atmospherically relevant as possible (low BVOC concentrations, high humidity), but the light intensities used were likely high enough to inhibit peroxy radical interactions that normally occur in the ambient environment.[52] Thus, we do not recommend using the SOA yields presented here for direct model integration. Rather, they are used here as a useful metric for comparing SOA formation potential between the different experiments. The integrated OH exposure inside the OFR ranged from 6.8×10^{11} to 9.8×10^{11} molecules cm^{-3} s in all trials. The corresponding equivalent of atmospheric photochemical age of this OH exposure range is 5−8 days assuming an ambient OH concentration of 1.5×10^6 molecules cm^{-3}.[60] In all trials, we assumed ΔBVOC was equal to the inlet concentration (e.g., we assumed all BVOCs reacted) which is a reasonable assumption for the conditions in this study; approximately 530 $\mu g\ m^{-3}$ of α-pinene could react (given OH rate constants 5.23×10^{-11} $cm^3\ molec^{-1}\ s^{-1}$)[61] at these OH exposure ranges, which is much higher than the measured BVOC inlet concentrations (14−190 $\mu g\ m^{-3}$). ΔC_{OA} was calculated from SMPS particle size distributions measured at the OFR outlet assuming a background condensed organic aerosol mass of zero (verified before starting each trial) and using a particle density of 1.4 g cm^{-3}, a reasonable value for laboratory biogenic SOA, which has been measured from 1.2 to 1.4 g cm^{-3}.[59,62,63]

2.4. Leaf Sample Collection, Preparation, and Metabolite Extraction. Leaves were harvested from plants at the end of each SOA trial. From each plant in the enclosure, 4−7 "sunlit" leaves (meaning leaves at the top of the plant) from each control and aphid-treated plant were harvested and immediately frozen in liquid N_2. Sunlit leaves at the top of the plant were targeted to eliminate known variability between sun and shade leaves, although it should be noted that these plants were small enough that all leaves were exposed to sunlight. The leaves at the top of the plant are the youngest leaves, but all leaves on these *Baccharis Salicifolia* plants were less than 6 months in age because all plants were grown from cuts collected in October of 2017. These samples were lyophilized, ground with a vibration bead mill Qiagen TissueLyzer II (Germantown, MD, U.S.A.) and stored at −80 °C until metabolite extraction. Polar and semipolar compounds were extracted following t'Kind et al. (2008) with minor modifications.[64] Briefly, for each sample, 30 mg of lyophilized powder was introduced into a 2 mL glass vial and 1 mL of methanol/water (80:20) was subsequently added. Samples were shaken for 1 h at 1000 rpm in a Thermoximer at 18 °C, centrifuged for 5 min at 12,000×*g*, and 0.8 mL of supernatants were split and transferred into two different sets of clean 2 mL tubes (0.3 mL for LC-MS and 0.5 mL for GC-MS). LC-MS analysis was performed directly on the methanol/water extracts using a high-resolution LTQ Orbitrap Velos mass spectrometer (HRMS) equipped with a heated electrospray ionization source (HESI) and coupled to a liquid chromatographer Vanquish ultrahigh pressure (UHPLC) (Thermo Fisher Scientific, Waltham, Massachusetts, U.S.A.). Additional details of chromatography, data filtering, and data analysis methods for GC-MS and LC-MS analysis are provided in Supporting Information (Section 2).

2.5. Statistical Analyses. After data filtering, the metabolomics data set containing both LC-MS and GC-MS foliar metabolome data was composed of one categorical factor with two levels: (control (C1, C2, C3, and C4 trials) and aphid (A1, A2, A3, and A4 trials) treated plants), and 25 001 continuous dependent variables (metabolomic features) where 218 metabolomic features were assigned a metabolite ID (Table S2). The TD-GC-MS data set of the identified plant volatile compounds was composed of a categorial factor with two levels (control (C1, C2, C3, and C4 trials) and aphid (A1, A2, A3, and A4 trials) treated plants) and 13 continuous variables (BVOC compounds). The foliar metabolome and BVOC emission profile of all plants contained in the enclosure for the SOA trial was used for tests of statistical difference between treatment and control.

Variability in the BVOC emission profile and foliar metabolome between control and aphid plants were visualized with a principal component analysis (PCA). PCA of the foliar metabolome was performed using data from individual plants within each trial to visualize intra- and inter-trial variability. PCA of the BVOC emission profiles was performed using the average from the SOA trial because emissions from individual plants were not measured. Differences in the BVOC emission profile and foliar metabolome between control and aphid plants were tested with permutational multivariate analysis of variance (PERMANOVA). Linear regressions were used to fit the SOA yield plots. All statistical analyses were performed using R (version 3.6.1) except for the linear regression, which was performed in Igor Pro software from WaveMetrics Inc. (version 7.0.2.2). The adonis function from the "vegan" package was used for PERMANOVAs.[65] PCAs were plotted using the PCA function from "FactoMineR" package.[66]

3. RESULTS AND DISCUSSION

3.1. Effect of Aphids on the Foliar Metabolome. The foliar metabolome was characterized to assess whether or not aphid herbivory affected the overall plant metabolome. Aphid herbivory altered the overall foliar metabolome (PERMANOVA; $p < 0.05$; Table S5). Principal component (PC)1 and PC2 of the PCA explained 47.9% (PC1 = 32.45% and PC2 = 15.45%) of the total variance and aphid herbivory and control treatments were clustered separately along the PC1 axis (Figure 3). PCA revealed larger metabolome variability between control plants than aphid plants along the PC2. In particular, we found that the total amino acid signal was significantly ($p < 0.01$) increased in aphid-treated plants compared to control groups (Table S7). Individual amino acids that significantly increased in treated plants include proline, histamine, adenine, asparagine, serine, aspartic acid, and tryptophan. Amino acids play important roles in plant stress response including regulating ion transport, modulating stomatal conductance, affecting synthesis and regulation of enzymes, gene expression, and participating in redox-homeostasis.[67] The relative abundance of jasmonic acid (JA), a common stress signaling hormone associated with insect herbivory,[68−71] was increased in aphid plants as well. These results demonstrate that aphid herbivory did affect the plant secondary metabolism and confirm the aphid treatment approach successfully induced an overall plant metabolic response.

https://doi.org/10.1021/acsearthspacechem.0c00300
ACS Earth Space Chem. 2021, 5, 1242−1253

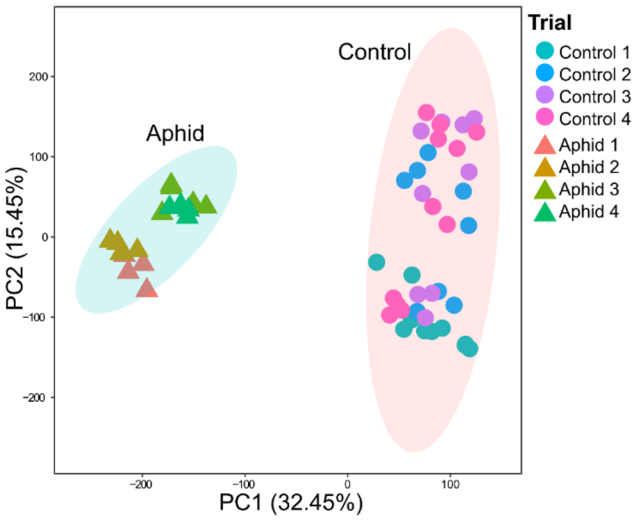

Figure 3. PCA of foliar metabolites from control (circles) and aphid (triangles) plants. Individuals included within each trial are represented in different color. Ellipses represent the distribution at 95% confidence interval for each of the treatments in the plane defined by both PC1 and PC2.

3.2. Effect of Aphids on the Gas-Phase BVOC Emission Profile. Unlike the foliar metabolome, the BVOC emission profile of control and aphid plants did not exhibit clear clustering based on treatment in a PCA (Figure 4),

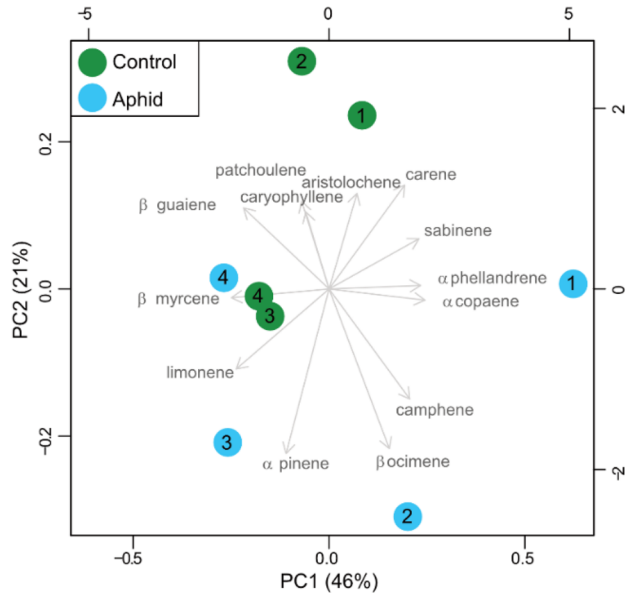

Figure 4. Biplot of the PCA of the gas-phase BVOC profile for control and aphid Baccharis trials. Circles represent the average BVOC profile from SOA trials. Numbers 1−4 indicate the experimental ID number (Table 1).

indicating that aphid herbivory did not have a clear effect on the BVOC emission profile (or the composition of the BVOCs emitted from the plants). PC1 and PC2 of the PCA explained a total variance of 67% (PC1 = 46% and PC2 = 21%). PC1 variability was largely explained by the relative contribution of α-copaene, sabinene, α-phellandrene, camphene, 3-carene, β-ocimene, and by β-guaiene. Variability along PC2 was explained mainly by the relative contribution of 3-carene, aristolochene, patchoulene, β-guaiene, β-ocimene, α-pinene, and camphene. On the basis of Figure 4, it is clear that there was substantial variation within treatment and control groups. Consistent with the PCA results, there was no significant difference between the BVOC emission profile of control and aphid plants as tested with PERMANOVA analysis (Table S6). This result is in contrast to some other plant-herbivore systems that have been studied previously where significant changes in the BVOC emission profile have been observed after herbivory. For example, gypsy moth herbivory altered the BVOC emission profile of holm oak by increasing β-caryophyllene emissions and inducing new sesquiterpene emissions such as α-humulene and δ-cadinene.[72] Aphid herbivory significantly increased emissions of monoterpenes like linalool and β-ocimene, and sesquiterpenes, such as α-farnesene or β-caryophyllene in European beech and tall fescue grasses.[73,74] On the basis of these previous studies from other plant-herbivore systems, our results were unexpected. We highlight that our results do not suggest the BVOC emission rates were unaffected by aphid herbivory; aphid herbivory has been documented to significantly increase BVOC emission rates from *Baccharis salicifolia*.[44] Indeed, it is likely that BVOC emission rates did increase from the aphid-exposed plants in our study (although this was not directly measured) because we were able to use fewer plants in the enclosure for the aphid SOA trials than the control SOA trials to achieve the same SOA mass loadings. Our measurements were not focused on characterizing BVOC emission rates, but rather the BVOC emission profile and how changes in the composition affect SOA production. Regarding the aphid effect on the BVOC emission profile, the results from this study demonstrated there was just as much variation within treatment groups as between treatment groups (even though all of these plants had been propagated from the same source and were thus genetically identical), and there was no clear impact of the aphid herbivore on the BVOC emission profile. These results highlight the intraspecies variability in BVOC emission profiles, which has been a major challenge in developing predictive models of plant stress emissions following biotic stress.[69,75]

Although the overall BVOC emission profile did not show significant differences between aphid and control plants, there were statistically significant differences in relative emissions of two individual compounds. To illustrate this, the average relative contribution of individual BVOC compounds from aphid and control trials are shown (Figure 5). BVOC emissions of both control and aphid *B. salicifolia* were dominated by limonene. Aphid herbivory significantly increased the relative contribution of β-ocimene and slightly decreased the relative contribution of β-guaiene. The contribution of β-ocimene increased by over 5 times, from 1.72% to 8.72% of the total BVOCs ($p < 0.01$). These results are consistent with a previous study showing *B. salicifolia* emissions are generally dominated by limonene and that aphid herbivory increased β-ocimene emissions.[44] On the other hand, the contribution of β-guaiene was marginally reduced ($p < 0.1$) in aphid plants (5.42%) compared to the control group (9.67%).

3.3. Chemical Controls on SOA Formation. SOA mass yields were plotted for each SOA trial to compare SOA formation efficiency of the BVOC mixtures from each set of plants (Figure 6). For all trials, the mass yield increased with increased mass loading as expected based on gas-particle partitioning theory.[54,55] Normally, an SOA mass yield curve

https://doi.org/10.1021/acsearthspacechem.0c00300
ACS Earth Space Chem. 2021, 5, 1242−1253

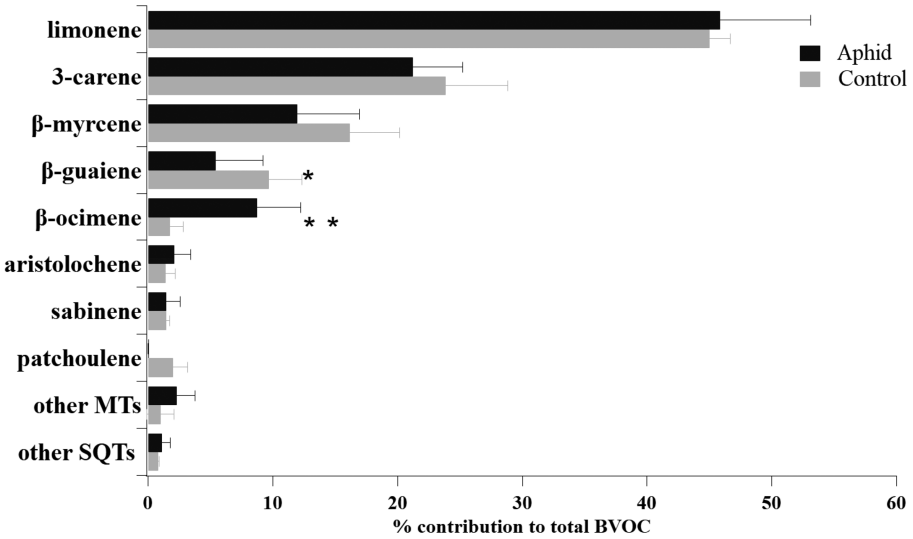

Figure 5. Average percent contribution of individual BVOC compounds during control and aphid Baccharis trials. Asterisk indicates significance level based on *t* test (*, $p < 0.1$ and **, $p < 0.01$). Other SQTs (sesquiterpenes) included caryophyllene and α-copaene. Other MTs (monoterpenes) included α-pinene, α-phellandrene, and camphene. Error bars denote the standard error of all cartridge samples.

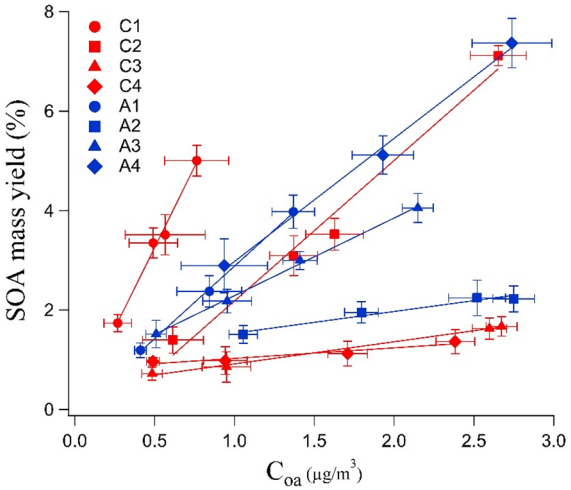

Figure 6. SOA mass yields for aphid and control trials. Lines represent best fits to the data using linear regression. C1−C4 denotes control trials and A1−A4 denotes aphid trials. Error bars denote standard deviation of the measurements.

would not exhibit linearity but would approach a maximum yield at higher condensed organic aerosol (C_{oa}) mass loadings. However, we targeted very low aerosol mass loadings to represent atmospherically relevant conditions in remote areas where BVOCs dominate SOA production, which means we stayed within the linear range of the mass yield curve rather than observing a yield threshold. The SOA yield threshold would typically occur at condensed mass concentrations at least an order of magnitude higher than those used in this study.[56] In both control and aphid trials, the SOA mass yield ranged from 1% to 7% across a condensed organic aerosol mass range of 0.5−3 μg m^{-3} in the OFR. These low-yield values were expected at the low mass loadings targeted in these trials; the estimated SOA mass yields from monoterpene-dominated BVOC mixtures ranged from 3% to 11% at similar organic aerosol mass loadings (0.5−6 μg m^{-3}).[76] Limonene and 3-carene are the dominant terpenes in the BVOC profile for all of the trials, collectively contributing 70−80% of total BVOCs by mass (Figure 5) and are likely driving a large fraction of the SOA production in the flow reactor. SOA mass yields of laboratory-generated limonene and 3-carene organic aerosols are less than 10% for condensed mass loadings below 10 μg m^{-3},[77,78] and thus these values are comparable with the yield values and corresponding organic aerosol mass values in this study.

SOA formation efficiency was defined as the slope of the line for each SOA mass yield curve; a steeper slope equals higher SOA formation efficiency. The slopes ranged from 0.44 to 2.91 and 0.21 to 6.49 for the aphid and control trials, respectively. This demonstrates there was as much variability in SOA formation efficiency within aphid/control groups as there was between groups. Recall from Section 3.2 that there was quite a bit of variability in the BVOC emission profiles between trials. Detailed BVOC emission profiles for each individual trial are provided in the Supporting Information to help explain some of the variability observed in SOA formation efficiency (Figure S1). The aphid 2 trial had the lowest SOA formation efficiency of all aphid plants and also had the smallest relative contribution from sesquiterpenes in the volatile profile. Aphid 3 and aphid 4 had nearly identical sesquiterpene contributions to the profile, but aphid 3 had a higher contribution from acyclic monoterpenes which can fragment upon oxidation and could explain the reduced SOA formation efficiency.[79] Of particular note, control 1 had the highest SOA formation efficiency with a slope of 6.49. The BVOC profile of the control 1 trial also had the highest cyclic-to-acyclic terpene ratio at 13% compared to the other trials which ranged from 2.7 to 6.5%. However, just qualitatively comparing the BVOC emission profiles of individual trials with the SOA formation efficiency does not indicate which molecular features were driving SOA formation from a more comprehensive perspective.

To systematically investigate relationships between BVOC structural class and SOA formation efficiency for all trials, we calculated the correlation between the slope of the SOA mass yield curve (e.g., the SOA formation efficiency) and the relative contribution of various compound classes and/or structures. This included relative fraction of cyclic terpenes, bicyclic

https://doi.org/10.1021/acsearthspacechem.0c00300
ACS Earth Space Chem. 2021, 5, 1242−1253

terpenes, monocyclic terpenes, total monoterpenes, total sesquiterpenes, and all individual compounds. The compounds were grouped as follows: bicyclic terpenes (aristolene, patchoulene, β-guaiene, caryophyllene, sabinene, 3-carene, camphene, α-pinene), acyclic terpenes (β-ocimene, β-myrcene), and monocyclic terpenes (limonene, α-phellandrene). A summary of these results is provided in Table 2. No single individual compound was correlated with SOA formation efficiency with correlations ranging from 0.03 to 0.50 (Table S8). Total sesquiterpene contribution was also not correlated with higher SOA formation efficiency. This is in contrast to results presented previously on the effects of bark borer herbivory on SOA mass yield from Scots pines where the sesquiterpene-to-monoterpene ratio was the primary predictor of SOA yield.[59] More recent studies have demonstrated that the large structural diversity in sesquiterpenes can produce different effects on aerosol formation and properties than would be expected if using β-caryophyllene as a model sesquiterpene compound.[80,81] These results further substantiate that sesquiterpene-to-monoterpene ratios cannot be used to estimate SOA mass yield, and that SOA production from a range of sesquiterpene structural classes should be the topic of future studies.

Table 2. Correlation between SOA Formation Efficiency and the Relative Contribution of Different Structural Classes to Total BVOCs

structural class	r^2
cyclic terpenes	0.82
bicyclic terpenes	0.61
monocyclic terpenes	0.08
monoterpenes	0.03
sesquiterpenes	0.03
individual terpenes	0.03−0.50

The highest correlation between SOA formation efficiency and BVOC structural class was observed in relation to the relative contribution of cyclic versus acyclic terpenes in the BVOC profile (r^2 = 0.82). Acyclic terpenes were negatively correlated with SOA formation efficiency (Figure 7). We note there could be a confounding relationship between SOA mass yield and OH exposure because we cannot control the OH exposure in the flow reactor with precision. Every effort was made to minimize variations in OH exposure by keeping the light settings the same throughout the experiment. We tested for any confounding relationship with OH exposure by plotting the cyclic-to-acyclic terpene contribution versus the OH exposure and confirmed there was no correlation (Figure S2). Thus, the relationship we observed between the proportion of cyclic terpenes to total BVOCs and SOA formation efficiency cannot be explained by small changes in OH exposure between the SOA trials. From a gas-phase chemistry perspective, a positive correlation between SOA formation efficiency and proportion of cyclic terpenes in the mixture makes sense; breaking endocyclic carbon−carbon double bonds results in ring-opening and retaining the carbon backbone while breaking carbon−carbon double bonds of acyclic compounds results in fragmentation of the molecule. Breaking the carbon−carbon bond at the location of the double bond is common during atmospheric oxidation of terpenes, which is why the dominant oxidation products of α-pinene are pinic acid and pinonic acid, both of which have a single ring while the parent compound, α-pinene, has a bicyclic molecular structure.[82] Fragmentation produces compounds with a smaller carbon backbone, by definition, and thus we would expect fragmentation reaction products from acyclic terpene oxidation to have higher volatility and lower SOA mass yields than ring-opening reaction products from cyclic terpene oxidation. This result is consistent with previous reports. The ozonolysis of Scots pine emissions containing a higher proportion of acyclic sesquiterpenes following aphid herbivory contained more fragmentation reaction products than the ozonolysis of healthy Scots pine emissions.[80] Furthermore, photooxidation of farnesene and bisabolene standards purchased from a chemical supplier have lower SOA mass yields than α-pinene.[81] Farnesene isomers are acyclic sesquiterpenes and bisabolene isomers are sesquiterpenes containing a long, unsaturated acyclic tail. These prior studies provided indirect evidence suggesting that an increased proportion of acyclic terpenes would be expected to decrease SOA mass yields, but this study is the first to more clearly link a reduction in SOA formation efficiency with an increasing proportion of acyclic terpenes in a complex BVOC mixture.

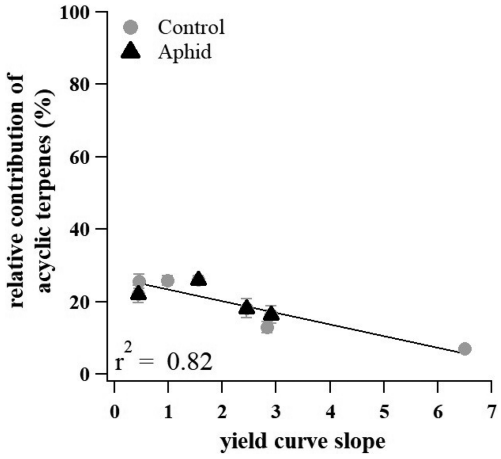

Figure 7. Correlation between the relative contribution of acyclic compounds to total BVOCs and SOA formation efficiency as defined as the SOA mass yield slope. Error bars denote the standard error.

4. CONCLUSION

This study characterized SOA formation potential of a complex mixture of BVOC emissions from a riparian shrub with and without being exposed to aphid herbivory. Foliar metabolome analysis indicated that aphid herbivory had a significant effect on plant metabolism, demonstrating the aphid herbivory treatment did influence plant metabolism and health. In particular, amino acids and jasmonic acid were elevated in aphid-exposed plants, both of which have been implicated in plant stress responses. In contrast, the BVOC emission profile was not significantly different between control and aphid plants. Overall, the BVOC emission profile exhibited a lot of variation between different sets of plants, regardless of aphid herbivory, and this led to measurable differences in the SOA formation potential between different BVOC mixtures. This provided the opportunity to examine the chemical controls on SOA formation related to differences in chemical composition of the BVOC mixture. The single chemical structural characteristic that was most correlated with SOA formation potential was the relative amount of cyclic-to-acyclic terpenes.

https://doi.org/10.1021/acsearthspacechem.0c00300
ACS Earth Space Chem. 2021, 5, 1242−1253

We found a negative correlation between the proportion of acyclic terpenes contributing to the BVOC mixture and the SOA formation efficiency. In this study, the relative contribution of acyclic terpenes to total BVOC emissions was not significantly altered by aphid herbivory. However, other studies have implicated acyclic terpenes as common inducible plant stress BVOCs following herbivory.[33,34,36] Currently, SOA models and chemical transport models do not explicitly account for the atmospheric chemistry of acyclic terpenes. Our results highlight the importance of acyclic terpenes in controlling SOA formation efficiency from a complex mixture, which could become even more prominent in an evolving world with increasing frequency and severity of plant stress conditions. Future studies should target a more comprehensive understanding of the atmospheric chemistry of acyclic terpene compounds including their effect on aerosol chemistry, formation, and climate-relevant properties.

■ ASSOCIATED CONTENT

Supporting Information

The Supporting Information is available free of charge at https://pubs.acs.org/doi/10.1021/acsearthspacechem.0c00300.

Details on gas-phase BVOC compound characterization using the TD-GC-ToF-MS, foliar metabolome characterization using GC-MS and LC-MS and related data processing and filtering; brief discussion about statistical analysis results, and plant volatile compounds distribution profile; MZmine parameter details and metabolite assignation information for metabolome (Tables S1 and S2, respectively); metabolite detector parameter details and metabolite assignation information for metabolome (Tables S3 and S4, respectively); summary results of PERMANOVA for metabolome and BVOC (Tables S5 and S6, respectively); student *t* test summary results for identified metabolites (Table S7); linear trendline r^2 value of yield curve versus relative contribution of individual BVOC to total BVOC (Table S8); plant BVOC distribution profiles of all trials (Figure S1); cyclic-to-acyclic BVOC ratio versus OH exposure curve (Figure S2) (PDF)

■ AUTHOR INFORMATION

Corresponding Author

Celia L. Faiola − *Department of Ecology and Evolutionary Biology and Department of Chemistry, University of California Irvine, Irvine, California 92697, United States;* orcid.org/0000-0002-4987-023X; Email: cfaiola@uci.edu

Authors

Farzaneh Khalaj − *Department of Ecology and Evolutionary Biology, University of California Irvine, Irvine, California 92697, United States*

Albert Rivas-Ubach − *Environmental Molecular Science Laboratory, Pacific Northwest National Laboratory, Richland, Washington 99352, United States;* orcid.org/0000-0003-1293-7127

Christopher R. Anderton − *Environmental Molecular Science Laboratory, Pacific Northwest National Laboratory, Richland, Washington 99352, United States;* orcid.org/0000-0002-6170-1033

Swarup China − *Environmental Molecular Science Laboratory, Pacific Northwest National Laboratory, Richland, Washington 99352, United States;* orcid.org/0000-0001-7670-335X

Kailen Mooney − *Department of Ecology and Evolutionary Biology, University of California Irvine, Irvine, California 92697, United States*

Complete contact information is available at: https://pubs.acs.org/10.1021/acsearthspacechem.0c00300

Notes

The authors declare no competing financial interest.

■ ACKNOWLEDGMENTS

A portion of the research was performed at the Environmental Molecular Sciences Laboratory, a U.S. Department of Energy National User Facility sponsored by the DOE Office of Science, Office of Biological and Environmental Research, which is located at Pacific Northwest National Laboratory (EMSL user proposal no. 49798). We also thank the University of California, Irvine (Ecology and Evolutionary Biology Doctoral Program) and the Ridge to Reef (R2R) Graduate Training Program funded by National Science Foundation Science Research Traineeship (NSF-NRT) award DGE-1735040.

■ REFERENCES

(1) Afendi, F. M.; Okada, T.; Yamazaki, M.; Hirai-Morita, A.; Nakamura, Y.; Nakamura, K.; Ikeda, S.; Takahashi, H.; Altaf-Ul-Amin, M.; Darusman, L. K.; Saito, K.; Kanaya, S. KNApSAcK Family Databases: Integrated Metabolite-Plant Species Databases for Multifaceted Plant Research. *Plant Cell Physiol.* **2012**, *53* (2), No. e1.

(2) Dudareva, N.; Klempien, A.; Muhlemann, J. K.; Kaplan, I. Biosynthesis, Function and Metabolic Engineering of Plant Volatile Organic Compounds. *New Phytol.* **2013**, *198* (1), 16−32.

(3) Knudsen, J. T.; Eriksson, R.; Gershenzon, J.; Ståhl, B. Diversity and Distribution of Floral Scent. *Bot. Rev.* **2006**, *72* (1), 1.

(4) Riccobono, F.; Schobesberger, S.; Scott, C. E.; Dommen, J.; Ortega, I. K.; Rondo, L.; Almeida, J.; Amorim, A.; Bianchi, F.; Breitenlechner, M.; David, A.; Downard, A.; Dunne, E. M.; Duplissy, J.; Ehrhart, S.; Flagan, R. C.; Franchin, A.; Hansel, A.; Junninen, H.; Kajos, M.; Keskinen, H.; Kupc, A.; Kürten, A.; Kvashin, A. N.; Laaksonen, A.; Lehtipalo, K.; Makhmutov, V.; Mathot, S.; Nieminen, T.; Onnela, A.; Petäjä, T.; Praplan, A. P.; Santos, F. D.; Schallhart, S.; Seinfeld, J. H.; Sipilä, M.; Spracklen, D. V.; Stozhkov, Y.; Stratmann, F.; Tomé, A.; Tsagkogeorgas, G.; Vaattovaara, P.; Viisanen, Y.; Vrtala, A.; Wagner, P. E.; Weingartner, E.; Wex, H.; Wimmer, D.; Carslaw, K. S.; Curtius, J.; Donahue, N. M.; Kirkby, J.; Kulmala, M.; Worsnop, D. R.; Baltensperger, U. Oxidation Products of Biogenic Emissions Contribute to Nucleation of Atmospheric Particles. *Science* **2014**, *344* (6185), 717−721.

(5) Ehn, M.; Thornton, J. A.; Kleist, E.; Sipila, M.; Junninen, H.; Pullinen, I.; Springer, M.; Rubach, F.; Tillmann, R.; Lee, B.; Lopez-Hilfiker, F.; Andres, S.; Acir, I.-H.; Rissanen, M.; Jokinen, T.; Schobesberger, S.; Kangasluoma, J.; Kontkanen, J.; Nieminen, T.; Kurten, T.; Nielsen, L. B.; Jørgensen, S.; Kjaergaard, H. G.; Canagaratna, M.; Maso, M. D.; Berndt, T.; Petaja, T.; Wahner, A.; Kerminen, V.-M.; Kulmala, M.; Worsnop, D. R.; Wildt, J.; Mentel, T. F. A Large Source of Low-Volatility Secondary Organic Aerosol | Nature. *Nature* **2014**, *506*, 476−479.

(6) Kiendler-Scharr, A.; Zhang, Q.; Hohaus, T.; Kleist, E.; Mensah, A.; Mentel, T. F.; Spindler, C.; Uerlings, R.; Tillmann, R.; Wildt, J. Aerosol Mass Spectrometric Features of Biogenic SOA: Observations from a Plant Chamber and in Rural Atmospheric Environments. *Environ. Sci. Technol.* **2009**, *43* (21), 8166−8172.

(7) Faiola, C. L.; Wen, M.; VanReken, T. M. Chemical Characterization of Biogenic Secondary Organic Aerosol Generated from Plant Emissions under Baseline and Stressed Conditions: Inter- and Intra-Species Variability for Six Coniferous Species. *Atmos. Chem. Phys.* **2015**, *15* (7), 3629−3646.
(8) Jimenez, J. L.; Canagaratna, M. R.; Donahue, N. M.; Prevot, A. S. H.; Zhang, Q.; Kroll, J. H.; DeCarlo, P. F.; Allan, J. D.; Coe, H.; Ng, N. L.; Aiken, A. C.; Docherty, K. S.; Ulbrich, I. M.; Grieshop, A. P.; Robinson, A. L.; Duplissy, J.; Smith, J. D.; Wilson, K. R.; Lanz, V. A.; Hueglin, C.; Sun, Y. L.; Tian, J.; Laaksonen, A.; Raatikainen, T.; Rautiainen, J.; Vaattovaara, P.; Ehn, M.; Kulmala, M.; Tomlinson, J. M.; Collins, D. R.; Cubison, M. J.; E Dunlea, J.; Huffman, J. A.; Onasch, T. B.; Alfarra, M. R.; Williams, P. I.; Bower, K.; Kondo, Y.; Schneider, J.; Drewnick, F.; Borrmann, S.; Weimer, S.; Demerjian, K.; Salcedo, D.; Cottrell, L.; Griffin, R.; Takami, A.; Miyoshi, T.; Hatakeyama, S.; Shimono, A.; Sun, J. Y.; Zhang, Y. M.; Dzepina, K.; Kimmel, J. R.; Sueper, D.; Jayne, J. T.; Herndon, S. C.; Trimborn, A. M.; Williams, L. R.; Wood, E. C.; Middlebrook, A. M.; Kolb, C. E.; Baltensperger, U.; Worsnop, D. R. Evolution of Organic Aerosols in the Atmosphere. *Science* **2009**, *326* (5959), 1525−1529.
(9) Zhao, D. F.; Buchholz, A.; Tillmann, R.; Kleist, E.; Wu, C.; Rubach, F.; Kiendler-Scharr, A.; Rudich, Y.; Wildt, J.; Mentel, T. F. Environmental Conditions Regulate the Impact of Plants on Cloud Formation. *Nat. Commun.* **2017**, *8*, 14067.
(10) Lambe, A. T.; Cappa, C. D.; Massoli, P.; Onasch, T. B.; Forestieri, S. D.; Martin, A. T.; Cummings, M. J.; Croasdale, D. R.; Brune, W. H.; Worsnop, D. R.; Davidovits, P. Relationship between Oxidation Level and Optical Properties of Secondary Organic Aerosol. *Environ. Sci. Technol.* **2013**, *47* (12), 6349−6357.
(11) Moise, T.; Flores, J. M.; Rudich, Y. Optical Properties of Secondary Organic Aerosols and Their Changes by Chemical Processes. *Chem. Rev.* **2015**, *115* (10), 4400−4439.
(12) Zhang, X.; Lin, Y.-H.; Surratt, J. D.; Zotter, P.; Prévôt, A. S. H.; Weber, R. J. Light-Absorbing Soluble Organic Aerosol in Los Angeles and Atlanta: A Contrast in Secondary Organic Aerosol. *Geophys. Res. Lett.* **2011**, *38*, L21810 DOI: 10.1029/2011GL049385.
(13) Guenther, A.; Karl, T.; Harley, P.; Wiedinmyer, C.; Palmer, P. I.; Geron, C. Estimates of Global Terrestrial Isoprene Emissions Using MEGAN (Model of Emissions of Gases and Aerosols from Nature). *Atmos. Chem. Phys.* **2006**, *6* (11), 3181−3210.
(14) Hallquist, M.; Wenger, J. C.; Baltensperger, U.; Rudich, Y.; Simpson, D.; Claeys, M.; Dommen, J.; Donahue, N. M.; George, C.; Goldstein, A. H.; Hamilton, J. F.; Herrmann, H.; Hoffmann, T.; Iinuma, Y.; Jang, M.; Jenkin, M. E.; Jimenez, J. L.; Kiendler-Scharr, A.; Maenhaut, W.; McFiggans, G.; Mentel, Th. F.; Monod, A.; Prévôt, A. S. H.; Seinfeld, J. H.; Surratt, J. D.; Szmigielski, R.; Wildt, J. The Formation, Properties and Impact of Secondary Organic Aerosol: Current and Emerging Issues. *Atmos. Chem. Phys.* **2009**, *9* (14), 5155−5236.
(15) Griffin, R. J.; Cocker, D. R.; Flagan, R. C.; Seinfeld, J. H. Organic Aerosol Formation from the Oxidation of Biogenic Hydrocarbons. *J. Geophys. Res. Atmospheres* **1999**, *104* (D3), 3555−3567.
(16) Odum, J. R.; Hoffmann, T.; Bowman, F.; Collins, D.; Flagan, R. C.; Seinfeld, J. H. Gas/Particle Partitioning and Secondary Organic Aerosol Yields. *Environ. Sci. Technol.* **1996**, *30* (8), 2580−2585.
(17) Ng, N. L.; Kroll, J. H.; Keywood, M. D.; Bahreini, R.; Varutbangkul, V.; Flagan, R. C.; Seinfeld, J. H.; Lee, A.; Goldstein, A. H. Contribution of First- versus Second-Generation Products to Secondary Organic Aerosols Formed in the Oxidation of Biogenic Hydrocarbons. *Environ. Sci. Technol.* **2006**, *40* (7), 2283−2297.
(18) Ng, N. L.; Chhabra, P. S.; Chan, A. W. H.; Surratt, J. D.; Kroll, J. H.; Kwan, A. J.; McCabe, D. C.; Wennberg, P. O.; Sorooshian, A.; Murphy, S. M.; Dalleska, N. F.; Flagan, R. C.; Seinfeld, J. H. Effect of NOx Level on Secondary Organic Aerosol (SOA) Formation from the Photooxidation of Terpenes. *Atmos. Chem. Phys.* **2007**, *7* (19), 5159−5174.
(19) Atkinson, R.; Arey, J. Atmospheric Chemistry of Biogenic Organic Compounds. *Acc. Chem. Res.* **1998**, *31* (9), 574−583.
(20) Atkinson, R.; Arey, J. Atmospheric Degradation of Volatile Organic Compounds. *Chem. Rev.* **2003**, *103* (12), 4605−4638.
(21) Loreto, F.; Dicke, M.; Schnitzler, J.-P.; Turlings, T. C. J. Plant Volatiles and the Environment. *Plant, Cell Environ.* **2014**, *37* (8), 1905−1908.
(22) Courtois, E. A.; Paine, C. E. T.; Blandinieres, P.-A.; Stien, D.; Bessiere, J.-M.; Houel, E.; Baraloto, C.; Chave, J. Diversity of the Volatile Organic Compounds Emitted by 55 Species of Tropical Trees: A Survey in French Guiana. *J. Chem. Ecol.* **2009**, *35* (11), 1349.
(23) Wieczynski, D. J.; Boyle, B.; Buzzard, V.; Duran, S. M.; Henderson, A. N.; Hulshof, C. M.; Kerkhoff, A. J.; McCarthy, M. C.; Michaletz, S. T.; Swenson, N. G.; Asner, G. P.; Bentley, L. P.; Enquist, B. J.; Savage, V. M. Climate Shapes and Shifts Functional Biodiversity in Forests Worldwide. *Proc. Natl. Acad. Sci. U. S. A.* **2019**, *116* (2), 587−592.
(24) Kulmala, M.; Suni, T.; Lehtinen, K. E. J.; Dal Maso, M.; Boy, M.; Reissell, A.; Rannik, U.; Aalto, P.; Keronen, P.; Hakola, H.; Back, J.; Hoffmann, T.; Vesala, T.; Hari, P. A New Feedback Mechanism Linking Forests, Aerosols, and Climate. *Atmos. Chem. Phys.* **2004**, *4* (2), 557−562.
(25) Kulmala, M.; Nieminen, T.; Chellapermal, R.; Makkonen, R.; Bäck, J.; Kerminen, V.-M. Climate Feedbacks Linking the Increasing Atmospheric CO2 Concentration, BVOC Emissions, Aerosols and Clouds in Forest Ecosystems. In *Biology, Controls and Models of Tree Volatile Organic Compound Emissions*; Niinemets, Ü., Monson, R. K., Eds.; Tree Physiology; Springer Netherlands: Dordrecht, 2013; pp 489−508.
(26) Arneth, A.; Harrison, S. P.; Zaehle, S.; Tsigaridis, K.; Menon, S.; Bartlein, P. J.; Feichter, J.; Korhola, A.; Kulmala, M.; O'Donnell, D.; Schurgers, G.; Sorvari, S.; Vesala, T. Terrestrial Biogeochemical Feedbacks in the Climate System. *Nat. Geosci.* **2010**, *3* (8), 525−532.
(27) Arneth, A.; Makkonen, R.; Olin, S.; Paasonen, P.; Holst, T.; Kajos, M. K.; Kulmala, M.; Maximov, T.; Miller, P. A.; Schurgers, G. Future Vegetation-Climate Interactions in Eastern Siberia: An Assessment of the Competing Effects of CO_2 and Secondary Organic Aerosols. *Atmos. Chem. Phys.* **2016**, *16* (8), 5243−5262.
(28) Guenther, A.; Hewitt, C. N.; Erickson, D.; Fall, R.; Geron, C.; Graedel, T.; Harley, P.; Klinger, L.; Lerdau, M.; Mckay, W. A.; Pierce, T.; Scholes, B.; Steinbrecher, R.; Tallamraju, R.; Taylor, J.; Zimmerman, P. A Global Model of Natural Volatile Organic Compound Emissions. *J. Geophys. Res.* **1995**, *100* (D5), 8873−8892.
(29) Rap, A.; Scott, C. E.; Reddington, C. L.; Mercado, L.; Ellis, R. J.; Garraway, S.; Evans, M. J.; Beerling, D. J.; MacKenzie, A. R.; Hewitt, C. N.; Spracklen, D. V. Enhanced Global Primary Production by Biogenic Aerosol via Diffuse Radiation Fertilization. *Nat. Geosci.* **2018**, *11* (9), 640.
(30) Wang, X.; Wu, J.; Chen, M.; Xu, X.; Wang, Z.; Wang, B.; Wang, C.; Piao, S.; Lin, W.; Miao, G.; Deng, M.; Qiao, C.; Wang, J.; Xu, S.; Liu, L. Field Evidences for the Positive Effects of Aerosols on Tree Growth. *Glob. Change Biol.* **2018**, *24* (10), 4983−4992.
(31) Wang, B.; Shugart, H. H.; Lerdau, M. T. Complexities between Plants and the Atmosphere. *Nat. Geosci.* **2019**, *12* (9), 693−694.
(32) Sporre, M. K.; Blichner, S. M.; Karset, I. H. H.; Makkonen, R.; Berntsen, T. K. BVOC-Aerosol-Climate Feedbacks Investigated Using NorESM. *Atmos. Chem. Phys.* **2019**, *19* (7), 4763−4782.
(33) Arneth, A.; Niinemets, Ü. Induced BVOCs: How to Bug Our Models? *Trends Plant Sci.* **2010**, *15* (3), 118−125.
(34) Holopainen, J. K.; Gershenzon, J. Multiple Stress Factors and the Emission of Plant VOCs. *Trends Plant Sci.* **2010**, *15* (3), 176−184.
(35) Niinemets, Ü. Mild versus Severe Stress and BVOCs: Thresholds, Priming and Consequences. *Trends Plant Sci.* **2010**, *15* (3), 145−153.
(36) Niinemets, Ü. Responses of Forest Trees to Single and Multiple Environmental Stresses from Seedlings to Mature Plants: Past Stress History, Stress Interactions, Tolerance and Acclimation. *For. Ecol. Manage.* **2010**, *260* (10), 1623−1639.
(37) Loreto, F.; Schnitzler, J.-P. Abiotic Stresses and Induced BVOCs. *Trends Plant Sci.* **2010**, *15* (3), 154−166.

(38) VanReken, T. M.; Greenberg, J. P.; Harley, P. C.; Guenther, A. B.; Smith, J. N. Direct Measurement of Particle Formation and Growth from the Oxidation of Biogenic Emissions. *Atmos. Chem. Phys.* **2006**, *6* (12), 4403−4413.
(39) Mentel, T. F.; Wildt, J.; Kiendler-Scharr, A.; Kleist, E.; Tillmann, R.; Dal Maso, M.; Fisseha, R.; Hohaus, T..; Spahn, H.; Uerlings, R.; Wegener, R.; Griffiths, P. T.; Dinar, E.; Rudich, Y.; Wahner, A. Photochemical Production of Aerosols from Real Plant Emissions. *Atmos. Chem. Phys.* **2009**, *9* (13), 4387−4406.
(40) Faiola, C. L.; Buchholz, A.; Kari, E.; Yli-Pirilä, P.; Holopainen, J. K.; Kivimäenpää, M.; Miettinen, P.; Worsnop, D. R.; Lehtinen, K. E. J.; Guenther, A. B.; Virtanen, A. Terpene Composition Complexity Controls Secondary Organic Aerosol Yields from Scots Pine Volatile Emissions. *Sci. Rep.* **2018**, *8* (1), 3053.
(41) Joutsensaari, J.; Yli-Pirilä, P.; Korhonen, H.; Arola, A.; Blande, J. D.; Heijari, J.; Kivimäenpää, M.; Mikkonen, S.; Hao, L.; Miettinen, P.; Lyytikäinen-Saarenmaa, P.; Faiola, C. L.; Laaksonen, A.; Holopainen, J. K. Biotic Stress Accelerates Formation of Climate-Relevant Aerosols in Boreal Forests. *Atmos. Chem. Phys.* **2015**, *15* (21), 12139−12157.
(42) Yli-Pirilä, P.; Copolovici, L.; Kännaste, A.; Noe, S.; Blande, J. D.; Mikkonen, S.; Klemola, T.; Pulkkinen, J.; Virtanen, A.; Laaksonen, A.; Joutsensaari, J.; Niinemets, Ü.; Holopainen, J. K. Herbivory by an Outbreaking Moth Increases Emissions of Biogenic Volatiles and Leads to Enhanced Secondary Organic Aerosol Formation Capacity. *Environ. Sci. Technol.* **2016**, *50* (21), 11501−11510.
(43) Mentel, Th. F.; Kleist, E.; Andres, S.; Dal Maso, M.; Hohaus, T.; Kiendler-Scharr, A.; Rudich, Y.; Springer, M.; Tillmann, R.; Uerlings, R.; Wahner, A.; Wildt, J. Secondary Aerosol Formation from Stress-Induced Biogenic Emissions and Possible Climate Feedbacks. *Atmos. Chem. Phys.* **2013**, *13* (17), 8755−8770.
(44) Moreira, X.; Nell, C. S.; Katsanis, A.; Rasmann, S.; Mooney, K. A. Herbivore Specificity and the Chemical Basis of Plant-Plant Communication in *Baccharis Salicifolia* (Asteraceae). *New Phytol.* **2018**, *220* (3), 703−713.
(45) Mooney, K. A.; Pratt, R. T.; Singer, M. S. The Tri-Trophic Interactions Hypothesis: Interactive Effects of Host Plant Quality, Diet Breadth and Natural Enemies on Herbivores. *PLoS One* **2012**, *7* (4), e34403.
(46) Dixon, A. F. G. Aphid Ecology: An Optimization Approach, **1998**. London, UK: Chapman & Hall.
(47) Ortega, J.; Helmig, D. Approaches for Quantifying Reactive and Low-Volatility Biogenic Organic Compound Emissions by Vegetation Enclosure Techniques - Part A. *Chemosphere* **2008**, *72* (3), 343−364.
(48) Hallquist, M.; Wenger, J. C.; Baltensperger, U.; Rudich, Y.; Simpson, D.; Claeys, M.; Dommen, J.; Donahue, N. M.; George, C.; Goldstein, A. H.; Hamilton, J. F.; Herrmann, H.; Hoffmann, T.; Iinuma, Y.; Jang, M.; Jenkin, M. E.; Jimenez, J. L.; Kiendler-Scharr, A.; Maenhaut, W.; McFiggans, G.; Mentel, T. F.; Monod, A.; Prévôt, A. S. H.; Seinfeld, J. H.; Surratt, J. D.; Szmigielski, R.; Wildt, J. The Formation, Properties and Impact of Secondary Organic Aerosol: Current and Emerging Issues. *Atmos. Chem. Phys.* **2009**, *9* (14), 5155−5236.
(49) Jimenez, J. L.; Canagaratna, M. R.; Donahue, N. M.; Prevot, A. S. H.; Zhang, Q.; Kroll, J. H.; DeCarlo, P. F.; Allan, J. D.; Coe, H.; Ng, N. L.; Aiken, A. C.; Docherty, K. S.; Ulbrich, I. M.; Grieshop, A. P.; Robinson, A. L.; Duplissy, J.; Smith, J. D.; Wilson, K. R.; Lanz, V. A.; Hueglin, C.; Sun, Y. L.; Tian, J.; Laaksonen, A.; Raatikainen, T.; Rautiainen, J.; Vaattovaara, P.; Ehn, M.; Kulmala, M.; Tomlinson, J. M.; Collins, D. R.; Cubison, M. J.; E Dunlea, J.; Huffman, J. A.; Onasch, T. B.; Alfarra, M. R.; Williams, P. I.; Bower, K.; Kondo, Y.; Schneider, J.; Drewnick, F.; Borrmann, S.; Weimer, S.; Demerjian, K.; Salcedo, D.; Cottrell, L.; Griffin, R.; Takami, A.; Miyoshi, T.; Hatakeyama, S.; Shimono, A.; Sun, J. Y.; Zhang, Y. M.; Dzepina, K.; Kimmel, J. R.; Sueper, D.; Jayne, J. T.; Herndon, S. C.; Trimborn, A. M.; Williams, L. R.; Wood, E. C.; Middlebrook, A. M.; Kolb, C. E.; Baltensperger, U.; Worsnop, D. R. Evolution of Organic Aerosols in the Atmosphere. *Science* **2009**, *326* (5959), 1525−1529.
(50) Zhang, Q.; Jimenez, J. L.; Canagaratna, M. R.; Allan, J. D.; Coe, H.; Ulbrich, I.; Alfarra, M. R.; Takami, A.; Middlebrook, A. M.; Sun, Y. L.; Dzepina, K.; Dunlea, E.; Docherty, K.; DeCarlo, P. F.; Salcedo, D.; Onasch, T.; Jayne, J. T.; Miyoshi, T.; Shimono, A.; Hatakeyama, S.; Takegawa, N.; Kondo, Y.; Schneider, J.; Drewnick, F.; Borrmann, S.; Weimer, S.; Demerjian, K.; Williams, P.; Bower, K.; Bahreini, R.; Cottrell, L.; Griffin, R. J.; Rautiainen, J.; Sun, J. Y.; Zhang, Y. M.; Worsnop, D. R. Ubiquity and Dominance of Oxygenated Species in Organic Aerosols in Anthropogenically-Influenced Northern Hemisphere Midlatitudes. *Geophys. Res. Lett.* **2007**, *34* (13), L13801.
(51) Lambe, A. T.; Ahern, A. T.; Williams, L. R.; Slowik, J. G.; Wong, J. P. S.; Abbatt, J. P. D.; Brune, W. H.; Ng, N. L.; Wright, J. P.; Croasdale, D. R.; Worsnop, D. R.; Davidovits, P.; Onasch, T. B. Characterization of Aerosol Photooxidation Flow Reactors: Heterogeneous Oxidation, Secondary Organic Aerosol Formation and Cloud Condensation Nuclei Activity Measurements. *Atmos. Meas. Tech.* **2011**, *4* (3), 445−461.
(52) Peng, Z.; Jimenez, J. L. Radical Chemistry in Oxidation Flow Reactors for Atmospheric Chemistry Research. *Chem. Soc. Rev.* **2020**, *49* (9), 2570−2616.
(53) Fröhlich, R.; Cubison, M. J.; Slowik, J. G.; Bukowiecki, N.; Prévôt, A. S. H.; Baltensperger, U.; Schneider, J.; Kimmel, J. R.; Gonin, M.; Rohner, U.; Worsnop, D. R.; Jayne, J. T. The ToF-ACSM: A Portable Aerosol Chemical Speciation Monitor with TOFMS Detection. *Atmos. Meas. Tech.* **2013**, *6* (11), 3225−3241.
(54) Odum, J. R.; Hoffmann, T.; Bowman, F.; Collins, D.; Flagan, R. C.; Seinfeld, J. H. Gas/Particle Partitioning and Secondary Organic Aerosol Yields. *Environ. Sci. Technol.* **1996**, *30* (8), 2580−2585.
(55) Pankow, J. F. An Absorption Model of Gas/Particle Partitioning of Organic Compounds in the Atmosphere. *Atmos. Environ.* **1994**, *28* (2), 185−188.
(56) Griffin, R. J.; Cocker, D. R.; Flagan, R. C.; Seinfeld, J. H. Organic Aerosol Formation from the Oxidation of Biogenic Hydrocarbons. *J. Geophys. Res. Atmospheres* **1999**, *104* (D3), 3555−3567.
(57) Ahlberg, E.; Falk, J.; Eriksson, A.; Holst, T.; Brune, W. H.; Kristensson, A.; Roldin, P.; Svenningsson, B. Secondary Organic Aerosol from VOC Mixtures in an Oxidation Flow Reactor. *Atmos. Environ.* **2017**, *161*, 210−220.
(58) Lambe, A. T.; Chhabra, P. S.; Onasch, T. B.; Brune, W. H.; Hunter, J. F.; Kroll, J. H.; Cummings, M. J.; Brogan, J. F.; Parmar, Y.; Worsnop, D. R.; Kolb, C. E.; Davidovits, P. Effect of Oxidant Concentration, Exposure Time, and Seed Particles on Secondary Organic Aerosol Chemical Composition and Yield. *Atmos. Chem. Phys.* **2015**, *15* (6), 3063−3075.
(59) Faiola, C. L.; Buchholz, A.; Kari, E.; Yli-Pirilä, P.; Holopainen, J. K.; Kivimäenpää, M.; Miettinen, P.; Worsnop, D. R.; Lehtinen, K. E. J.; Guenther, A. B.; Virtanen, A. Terpene Composition Complexity Controls Secondary Organic Aerosol Yields from Scots Pine Volatile Emissions. *Sci. Rep.* **2018**, *8*, 3053.
(60) Mao, J.; Ren, X.; Brune, W. H.; Olson, J. R.; Crawford, J. H.; Fried, A.; Huey, L. G.; Cohen, R. C.; Heikes, B.; Singh, H. B.; Blake, D. R.; Sachse, G. W.; Diskin, G. S.; Hall, S. R.; Shetter, R. E. Airborne Measurement of OH Reactivity during INTEX-B. *Atmos. Chem. Phys.* **2009**, *9* (1), 163−173.
(61) Atkinson, R.; Arey, J. Atmospheric Degradation of Volatile Organic Compounds. *Chem. Rev.* **2003**, *103* (12), 4605−4638.
(62) Malloy, Q. G. J.; Nakao, S.; Qi, L.; Austin, R.; Stothers, C.; Hagino, H.; Cocker, D. R. Real-Time Aerosol Density Determination Utilizing a Modified Scanning Mobility Particle Sizer—Aerosol Particle Mass Analyzer System. *Aerosol Sci. Technol.* **2009**, *43* (7), 673−678.
(63) Nakao, S.; Tang, P.; Tang, X.; Clark, C. H.; Qi, L.; Seo, E.; Asa-Awuku, A.; Cocker, D. Density and Elemental Ratios of Secondary Organic Aerosol: Application of a Density Prediction Method. *Atmos. Environ.* **2013**, *68*, 273−277.
(64) t'Kindt, R.; De Veylder, L.; Storme, M.; Deforce, D.; Van Bocxlaer, J. LC-MS Metabolic Profiling of Arabidopsis Thaliana Plant Leaves and Cell Cultures: Optimization of Pre-LC-MS Procedure Parameters. *J. Chromatogr. B: Anal. Technol. Biomed. Life Sci.* **2008**, *871* (1), 37−43.

(65) Oksanen, J.; Blanchet, F. G.; Friendly, M.; Kindt, R.; Legendre, P.; McGlinn, D.; Minchin, P. R.; O'Hara, R. B.; Simpson, G. L.; Solymos, P.; Stevens, M. H. H.; Szoecs, E.; Wagner, H. *Vegan: Community Ecology Package*; **2019**, https://CRAN.R-project.org/package=vegan.
(66) Husson, F.; Josse, J.; Le, S.; Mazet, J. *FactoMineR: Multivariate Exploratory Data Analysis and Data Mining* **2020**, *25* (1), 1−18.
(67) Rai, V. K. Role of Amino Acids in Plant Responses to Stresses. *Biol. Plant.* **2002**, *45* (4), 481−487.
(68) Leitner, M.; Boland, W.; Mithöfer, A. Direct and Indirect Defences Induced by Piercing-Sucking and Chewing Herbivores in Medicago Truncatula. *New Phytol.* **2005**, *167* (2), 597−606.
(69) Faiola, C.; Taipale, D. Impact of Insect Herbivory on Plant Stress Volatile Emissions from Trees: A Synthesis of Quantitative Measurements and Recommendations for Future Research. *Atmospheric Environ. X* **2020**, *5*, 100060.
(70) Wasternack, C. Jasmonates: An Update on Biosynthesis, Signal Transduction and Action in Plant Stress Response, Growth and Development. *Ann. Bot.* **2007**, *100* (4), 681−697.
(71) Staudt, M.; Jackson, B.; El-Aouni, H.; Buatois, B.; Lacroze, J.-P.; Poëssel, J.-L.; Sauge, M.-H.; Niinemets, Ü. Volatile Organic Compound Emissions Induced by the Aphid Myzus Persicae Differ among Resistant and Susceptible Peach Cultivars and a Wild Relative. *Tree Physiol.* **2010**, *30* (10), 1320−1334.
(72) Staudt, M.; Lhoutellier, L. Volatile Organic Compound Emission from Holm Oak Infested by Gypsy Moth Larvae: Evidence for Distinct Responses in Damaged and Undamaged Leaves. *Tree Physiol.* **2007**, *27* (10), 1433−1440.
(73) Joó, É.; Van Langenhove, H.; Šimpraga, M.; Steppe, K.; Amelynck, C.; Schoon, N.; Müller, J.-F.; Dewulf, J. Variation in Biogenic Volatile Organic Compound Emission Pattern of Fagus Sylvatica L. Due to Aphid Infection. *Atmos. Environ.* **2010**, *44* (2), 227−234.
(74) Li, T.; Blande, J. D.; Gundel, P. E.; Helander, M.; Saikkonen, K. Epichloë Endophytes Alter Inducible Indirect Defences in Host Grasses. *PLoS One* **2014**, *9* (6), No. e101331.
(75) Guenther, A. B.; Jiang, X.; Heald, C. L.; Sakulyanontvittaya, T.; Duhl, T.; Emmons, L. K.; Wang, X. The Model of Emissions of Gases and Aerosols from Nature Version 2.1 (MEGAN2.1): An Extended and Updated Framework for Modeling Biogenic Emissions. *Geosci. Model Dev.* **2012**, *5* (6), 1471−1492.
(76) Hao, L. Q.; Romakkaniemi, S.; Yli-Pirilä, P.; Joutsensaari, J.; Kortelainen, A.; Kroll, J. H.; Miettinen, P.; Vaattovaara, P.; Tiitta, P.; Jaatinen, A.; Kajos, M. K.; Holopainen, J. K.; Heijari, J.; Rinne, J.; Kulmala, M.; Worsnop, D. R.; Smith, J. N.; Laaksonen, A. Mass Yields of Secondary Organic Aerosols from the Oxidation of α-Pinene and Real Plant Emissions. *Atmos. Chem. Phys.* **2011**, *11* (4), 1367−1378.
(77) Draper, D. C.; Farmer, D. K.; Desyaterik, Y.; Fry, J. L. A Qualitative Comparison of Secondary Organic Aerosol Yields and Composition from Ozonolysis of Monoterpenes at Varying Concentrations of NO_2. *Atmos. Chem. Phys.* **2015**, *15* (21), 12267−12281.
(78) Friedman, B.; Farmer, D. K. SOA and Gas Phase Organic Acid Yields from the Sequential Photooxidation of Seven Monoterpenes. *Atmos. Environ.* **2018**, *187*, 335−345.
(79) Ziemann, P. J. Effects of Molecular Structure on the Chemistry of Aerosol Formation from the OH-Radical-Initiated Oxidation of Alkanes and Alkenes. *Int. Rev. Phys. Chem.* **2011**, *30* (2), 161−195.
(80) Faiola, C. L.; Pullinen, I.; Buchholz, A.; Khalaj, F.; Ylisirniö, A.; Kari, E.; Miettinen, P.; Holopainen, J. K.; Kivimäenpää, M.; Schobesberger, S.; Yli-Juuti, T.; Virtanen, A. Secondary Organic Aerosol Formation from Healthy and Aphid-Stressed Scots Pine Emissions. *ACS Earth Space Chem.* **2019**, *3* (9), 1756−1772.
(81) Ylisirniö, A.; Buchholz, A.; Mohr, C.; Li, Z.; Barreira, L.; Lambe, A.; Faiola, C.; Kari, E.; Yli-Juuti, T.; Nizkorodov, S. A.; Worsnop, D. R.; Virtanen, A.; Schobesberger, S. Composition and Volatility of Secondary Organic Aerosol (SOA) Formed from Oxidation of Real Tree Emissions Compared to Simplified Volatile Organic Compound (VOC) Systems. *Atmos. Chem. Phys.* **2020**, *20* (9), 5629−5644.
(82) Yu, J.; Griffin, R. J.; Cocker, D. R.; Flagan, R. C.; Seinfeld, J. H.; Blanchard, P. Observation of Gaseous and Particulate Products of Monoterpene Oxidation in Forest Atmospheres. *Geophys. Res. Lett.* **1999**, *26* (8), 1145−1148.

https://doi.org/10.1021/acsearthspacechem.0c00300
ACS Earth Space Chem. 2021, 5, 1242−1253